State-to-state reaction dynamics of R+HCN ($\nu_1 \nu_2^{l_2} \nu_3$)→RH+CN(v,J) with R=Cl, H

Christoph Kreher, Robert Theinl, and Karl-Heinz Gericke
Institut für Physikalische und Theoretische Chemie, der Johann Wolfgang Goethe-Universität, Marie-Curie-Strasse 11, D-60439 Frankfurt/Main, Germany

(Received 26 April 1995; accepted 7 November 1995)

Vibrational overtone excitation of HCN in the wavelength region 6 500 cm^{-1}–18 000 cm^{-1} is used to initiate the endothermic reaction of chlorine and hydrogen atoms with HCN. HCN is excited to the overtone levels (002), (004), (302), (105), and ($11^1$5). The labeling of the vibrational levels ($\nu_1 \nu_2^{l_2} \nu_3$) corresponds to the normal modes ν_1=CN, ν_2=bend, ν_3=CH, and l_2=vibrational angular momentum. The product state distribution of CN($X\ ^2\Sigma^+$) is completely analyzed by laser induced fluorescence (LIF). Excitation of the first overtone of CH-stretch leads to vibrationally excited CN in the reaction of Cl+HCN(002), implying the existence of a long living complex. The CN vibrational excitation increases with increasing H–CN stretch excitation. However, a slightly higher CN vibrational excitation is found when at the same internal energy of HCN three quanta of CN-stretch and two quanta of CH-stretch are excited. Therefore, the energy is not completely redistributed in the collision complex. The ratio of rate constants between the reactions of HCN(004) and HCN(302) with Cl is 2.8±0.6. The CN product vibrational excitation decreases again, when HCN is excited to the (105) state. At these high HCN vibrational energies the reaction mechanism seems to change toward a more direct reaction where the time left is not sufficient for energy randomization. The reaction of hydrogen with HCN(004) leads to CN-products with a similar vibrational distribution, as in the case of chlorine, but with a lower rotational excitation. The reaction H+HCN(302) shows no significant generation of CN products and a lower limit of the ratio of rate constants, $k(004)/k(302)>4$, is obtained. © *1996 American Institute of Physics.* [S0021-9606(96)00607-4]

I. INTRODUCTION

One important goal in molecular dynamics is the understanding how the initially populated rovibrational states of the reactants influence the reaction rate and the state distribution of the products. In this study the rules for reagent energy consumption (vibration and translation) and product energy release are investigated for an atom plus triatom systems,

$$A+BCD(\nu_1,\nu_2,\nu_3)\rightarrow AB+CD(v,J),$$

by exciting the molecular reagent in different vibrational modes (ν_1,ν_2,ν_3) and by using different photolysis wavelengths for the generation of the atomic collision partner. The influence of the vibrational modes on the reaction rate and on the energy disposal is investigated.

The following endothermic reactions of hydrogen and chlorine atoms with HCN have been analyzed:

$$HCN(\tilde{X}\ ^1\Sigma^+)+Cl(^2P)\rightarrow HCl(X\ ^1\Sigma^+)+CN(X\ ^2\Sigma^+)$$

$$\Delta_r H^{298}=94\ \text{kJ/mol}, \quad (1)$$

$$HCN(\tilde{X}\ ^1\Sigma^+)+H(^2S)\rightarrow H_2(X\ ^1\Sigma^+)+CN(X\ ^2\Sigma^+)$$

$$\Delta_r H^{298}=90\ \text{kJ/mol}. \quad (2)$$

The total reaction barrier of Cl+HCN is about 113 kJ/mol.[1] Smith and co-workers have measured the rates of the reverse reaction (1), CN+HCl→products, by exciting either the CN or the HCl vibration.[2] While one quantum of vibration in the CN has no effect on the reaction rate, the rate is increasing by more than two orders of magnitude when HCl is excited in the first vibrational state. This implies that CN behaves like an atom, i.e., the internal motion of the CN is unimportant for the reaction rate. Only the bond that will be broken (H–Cl) promotes the reaction. According to the simple picture of an atom exchange reaction, A+BC→AB+C, a late reaction barrier can be expected. If CN+HCl generates Cl +HCN, then the results of Smith and co-workers may suggest that in the present study CN should be formed with low vibrational excitation when the CN bond in HCN is not excited. One result of this work will be that the picture of a CN spectator during the course of the reaction is too simple to describe the dynamics.

The reaction of H+HCN is endothermic by 90 kJ/mol. Schacke *et al.*[3] determined an activation energy of 22±3 kJ/mol, thus the total activation energy for this reaction lies between 109 and 115 kJ/mol. Lambert *et al.*[4] have analyzed the reaction by using translationally hot H atoms. Precursors of the H atoms were H_2S and HBr, photolyzed at 193 nm leading to available energies of 132 kJ/mol and 153 kJ/mol for the H_2+CN products. Their observed CN state distribution is characterized by a relatively high rotational and low vibrational energy release which supports the assumption of a linear transition state as already suggested by former *ab initio* calculations.[5] The rate of the reverse reaction, H_2+CN, is observed to be uneffected by vibrationally excited CN.[6] However, vibrational excitation of H_2 should increase the

TABLE I. Band origins ν_0 (cm^{-1}), absolute intensities A ($cm\ mol^{-1}$), and excitation conditions for different overtone bands of HCN.

Overtone	ν_0/cm^{-1}	λ/nm	$A/cm\ mol^{-1}$	Pulse energy dye
(002)← (000)	6 519.61[a]	1533.4	$8.499(54)\times10^4$ [a]	15 mJ DCM[e]
(004)← (000)	12 635.89[a]	791.18	157(1),[a] 154(2)[b]	40 mJ LDS 765
(302)← (000)	12 657.88[a]	789.81	9.11(25),[a] 9.7(2)[b]	40 mJ LDS 765
(005)← (000)	15 551.94[a]	642.83	17.5(4)[a]	100 mJ DCM
$(11\ ^1 5)\leftarrow(01\ ^1 0)$	17 449.30[c]	572.93	3.70(11)[c]	120 mJ R6G
(105)← (000)	17 550.42[d]	569.63	3.51(17),[c] 13.9(4)[a]	120 mJ R6G

[a]Reference 10.
[b]Reference 12.
[c]Reference 14.
[d]Reference 15.
[e]Frequency mixing with 1.064 μm.

reaction rate according to theoretical studies.[7] These findings suggest—comparable to the reaction HCl+CN→HCN +Cl—that in the reaction of hydrogen atoms with HCN, H+HCN→H_2+CN, the CN bond is unaffected during the reactive encounter.

The influence of vibrational motion in HCN on the reaction dynamics is investigated by IR/VIS excitation of several vibrational bands,[8–15]

$$\mathrm{HCN}(J,v_1=0,v_2=0,v_3=0)+h\nu\rightarrow\mathrm{HCN}(J',v_1',v_2',v_3'). \tag{3}$$

Spectroscopic studies of HCN have been performed by many research groups because of its significance in chemical physics and astrophysics. We follow Herzberg's convention for labeling the vibrational modes of HCN ($\nu_1\nu_2^{l_2}\nu_3$); ν_1 is the CN stretch, ν_2 is the degenerate bending mode, ν_3 is the CH stretch, and l_2 is the vibrational angular momentum. In the case of $\nu_2=0$ the quantum number l_2 is not further given. Excitation of one rotational state of the overtone levels (002), (004), (302), (105), and (11^15) of HCN were used to initiate the reaction with chlorine atoms. The reaction of hydrogen atoms was studied with HCN in the (004) and (302) states. In the case that different vibrational bands of HCN lie within the tuning range of the excitation laser, we could determine a ratio of rate constants between those different vibrational states. Table I gives a summary of all vibrational bands used here, together with their band origins and absolute intensities.

II. EXPERIMENT

HCN is conventionally prepared by heating a mixture of KCN and stearic acid in vacuum to ~100 °C. The gaseous product is trapped in a bulb at 77 K. Preparing HCN following this prescription should be free of dicyan.[16]

Chlorine atoms were generated from Cl_2 in a pulsed laser photolysis at 308 nm (Lambda Physik MSC101) and 355 nm (Quanta Ray DCR1A). The pulse energies were typically 20–40 mJ.

To avoid a reaction of hydrogen with thermal HCN, the collision energy of H+HCN, which is essentially the translational energy of H, must be lower than 110 kJ/mol. Photodissociating of methanthiol at 266 nm appears to be the appropriate precursor because the H atoms are generated at relatively low mean translational energies of 80 kJ/mol. The width of the energy distribution is also very narrow (see Sec. III). Furthermore, the photodecomposition at 266 nm has a high absorption cross section of $\sigma=4\times10^{-20}$ cm^2 and yields exclusively H atoms. Break of the stronger SH bond is preferred for long wavelength photolysis, while the CS bond breaks below λ=222 nm. At 193 nm it equally competes with the SH cleavage.[17,18,19] The methanthiol in the present study was photolyzed at 266 nm generated from the fourth harmonic (15 mJ) of a Nd:YAG laser.

To avoid any reactions of CH_3SH/Cl_2 with HCN prior to photolytic initiation, the reactants were mixed in the reaction chamber by separate nozzles. The chamber was evacuated by an oil diffusion pump, reaching a base pressure of $\sim10^{-2}$ Pa. The partial pressures were $P(Cl_2)=8$ Pa and $P(CH_3SH)=P(HCN)=16$ Pa.

Probing the (002)←(000) overtone band of HCN in the infrared region was performed via difference frequency mixing of a dye laser and a 1.064 μm Nd:YAG laser beam (Continuum YG 680, TDL 60, IRP). The dye laser operated with DCM at an output energy of 80 mJ at 627 nm. The beams were mixed in a lithium niobate crystal and an automatic wavelength tracking system was used to maintain the optimum conversion efficiency when the laser was tuned. The IR-output around 1530 nm was separated from the residual radiation at 627 nm and 1.064 μm by a CaF_2 Pellin Broca prism. All other wavelengths in the visible and near infrared region were obtained using different laser dyes (Table I). The pulse width of the laser was typically 7 ns at a bandwidth (FWHM) of 0.07–0.09 cm^{-1} (Table I). In the case of the (302)←(000) excitation we used the $P(8)$ line, in all other cases the $R(8)$ transition was used to initiate the reaction of HCN with H/Cl.

To exclude any other reactions producing CN than the desired reactions of H or Cl atoms with vibrationally excited HCN, we tried to measure CN spectra with HCN exclusively or with HCN+Cl_2/CH_3SH but without firing the HCN excitation laser. In both cases the CN-background signal was negligible small or no signal could be detected. At the photolysis wavelengths of 266 nm and 308 nm a small amount of CN was detected from direct photodissociation of the pre-

excited HCN sample. However, this background signal was extremely weak and no correction for the CN resulting from the bimolecular reactions of Cl/H with HCN was necessary.

The CN($X\ ^2\Sigma^+$) product of the reaction channels (1) and (2) were monitored by the laser induced fluorescence technique (LIF).[20,21] The nascent CN state distribution was probed via the $B\ ^2\Sigma^+ \leftarrow X\ ^2\Sigma^+$ ($\Delta v = 0$) band using a dye laser (Lambda Physik FL2002, QUI) pumped by a XeCl excimer laser (Lambda Physik EMG 101 MSC). All LIF spectra were detected with 2–5 mJ of laser light under saturated conditions. A photomultiplier (THORN-EMI 9781B) monitored the LIF signal perpendicular to the probe beam through f/1 optics. To reduce scattered light from the laser beams, the LIF signal was spectrally filtered by an interference filter (389 ± 10 nm). Furthermore the reaction chamber was equipped with 50 cm sidearms which contained baffles. All three laser beams were aligned parallel to each other where the HCN pump beam was counter propagating the photolysis and probe beam. The beams were focused by 50 cm lenses. In the case of the CH_3SH photolysis at 266 nm, a 100 cm lens was used to avoid two photon absorption of HCN. A boxcar integrator (Stanford Research system, DG 535) interfaced to a computer processed the signal. The lasers operated at a repetition rate of 10 Hz. The time delay between the photolysis laser—which is in time with the IR/VIS excitation laser—and the LIF-probe laser was set to 150 ns.

An optional mirror could be used to direct the HCN excitation beam into a photoacoustic cell which determines when the IR/VIS laser frequency corresponds to a rovibrational transition in HCN. The same experimental set up was also used to measure the spectral width of the IR laser ($\Delta\nu \approx 0.08\ \mathrm{cm}^{-1}$) because the absorption lines for (002)←(000) transitions of HCN are very narrow ($\Delta\nu < 0.02\ \mathrm{cm}^{-1}$).

III. RESULTS

A. Energetics

The 308 nm and 355 nm photolysis of Cl_2 produces Cl atoms essentially in the energetically lowest spin–orbit state, $^2P_{3/2}$. We performed calculations for the center of mass collision energy distribution of the Cl+HCN system by using an excess energy of $E_{\mathrm{exc}}(\mathrm{Cl}) = \frac{1}{2}[E_{h\nu}(308/355\ \mathrm{nm}) + E_{\mathrm{int}}(\mathrm{Cl_2}) - D_0(\mathrm{Cl–Cl})]$. The calculations were performed on the basis of the works of Chantry[22] and van der Zande *et al.*,[23] where an analytical expression for the collision energy distribution in hot atom reactions for a fixed excess energy is presented. In addition, we integrated these expressions over the excess energy distribution resulting from the internal energy of the Cl_2 molecule in order to obtain the final collision energy distribution for the Cl+HCN system. The mean collision energy is $E_{\mathrm{coll}} = 25\ \mathrm{kJ\ mol}^{-1}$ for the photolysis at 355 nm and 36 kJ mol^{-1} at 308 nm. The spread in the collision energy distribution arises not only from the thermal translational motions of the reactants but also from the internal energy distribution of the Cl_2 precursor molecule. Figure 1 shows the collision energy distribution of the Cl +HCN reaction system. Obviously, the reaction rate of HCN in the vibrational ground state must be negligibly small due to energy reasons. We calculated the amount of chlorine atoms for the photolysis at 308 nm (355 nm) which have suffered just one collision within the 150 ns delay time to be 74% (84%). Thus, at most 26% (16%) of all chlorine atoms may exhibit a different collision energy distribution than the one shown in Fig. 1 due to nonreactive collisions in the "first Cl+HCN encounter." Therefore, the major part of all observed CN products must be generated via an energy distribution shown in Fig. 1.

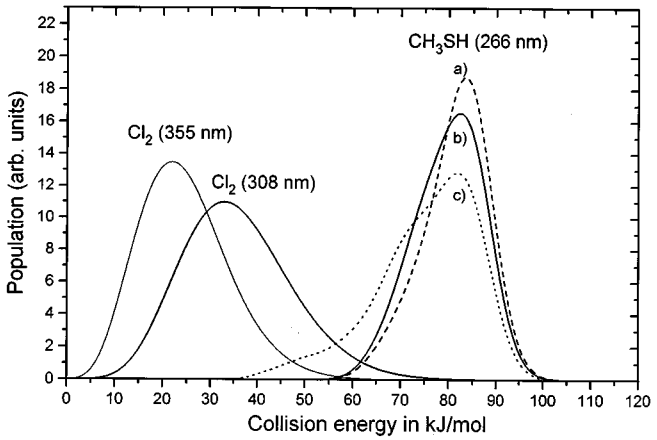

FIG. 1. Distributions of the collision energies for the systems H+HCN and Cl+HCN. The collision energy distribution of H+HCN (curve b) has been calculated using the measured internal energy distributions of CH_3S at a photolysis wavelength of 274 nm (dashed curve a) and at 243.3 nm (dotted curve c) (Ref. 19). The internal energy of CH_3S at the photolysis wavelength of 266 nm has been obtained by interpolation of the two CH_3S internal energy distribution at the measured wavelengths.

For the reaction of hydrogen atoms with HCN the excess energy is calculated according to $E_{\mathrm{exc}}(\mathrm{H}) = E_{h\nu}(266\ \mathrm{nm}) + E_{\mathrm{int}}(\mathrm{CH_3SH}) - E_{\mathrm{int}}(\mathrm{CH_3S}) - D_0(\mathrm{CH_3S–H})$. While in our calculations the mean internal energy of the CH_3SH molecule is fixed to $3/2RT$, we used different energy distributions of the CH_3S fragment derived from works of Wilson *et al.*[24] and Jensen *et al.*[25] They measured the internal energy distribution of the CH_3S radical at different fixed UV photolysis wavelengths of CH_3SH. Using their results, we performed calculations of the collision energy distribution of the H+HCN reaction, where the H atom is generated at a photolysis wavelength of 266 nm. In the first case [Fig. 1(a)] we integrated over the internal energy distribution of CH_3S arising from the photolysis of CH_3SH at 274 nm and in the second case [Fig. 1(c)] integration was performed over the CH_3S internal energy distribution from the 243.3 nm photolysis. Because both internal energy distributions of CH_3S do not exactly describe the distribution at a photodissociation wavelength of 266 nm light, we interpolated the energy release in the CH_3S fragment for this wavelength. The resulting H+HCN collision energy distribution is shown in Fig. 1(c). Roughly 7.7% of the excess energy is located as internal energy in the CH_3S radical. The collision energy distribution is characterized by a mean energy of 80 kJ/mol at a spread of 18 kJ/mol. Similar to the Cl+HCN reaction the major part of all observed CN products is generated via the

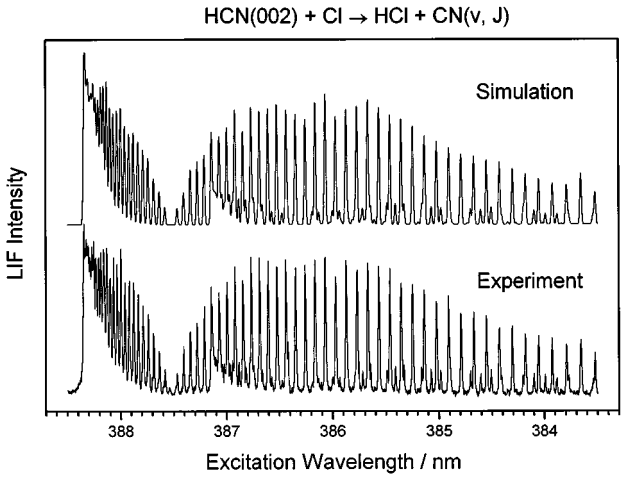

FIG. 2. Laser induced fluorescence spectrum of CN generated in the reaction of chlorine atoms with HCN where 2 CH stretch quanta of HCN are excited (lower part). For an evaluation of the experimental spectrum a simulation of the spectrum has been performed (upper part).

energy distribution shown in Fig. 1 because the contribution of translationally relaxed H atoms is small.

In another experiment the translationally hot H atoms were cooled down to room temperature by adding helium to the CH_3SH/HCN mixture. In that case a Boltzmann distribution of the collision energy is assumed for the H+HCN reaction system. It should be mentioned that the HCN may also be influenced by collisions with helium because the timing between CH_3SH photolysis and HCN pre-excitation could not be varied.

B. Cl+HCN(ν_1,ν_2,ν_3)

The complete CN product state distribution is obtained by probing the rovibrational transitions of the $B\ ^2\Sigma^+ \leftarrow X\ ^2\Sigma^+$ system. Simulations of the CN spectrum were used to fit all observed rotational lines. The first important result is that each rotational distribution can be well characterized by a rotational temperature. The reaction of Cl with HCN(ν_3=2) (Fig. 2) leads to vibrationally excited CN with population ratios of $P(v=0):P(v=1):P(v=2)$ $=86\%:13\%:<1\%$. The rotational distributions for $v=0$ and $v=1$ are characterized by the temperature parameters of 1700 K and 945 K, respectively. The characteristic quantities of the CN product state distributions are listed in Table II.

The influence of increasing CH stretch motion of HCN on the reaction is analyzed by exciting $4\nu_{CH}$ quanta. The simulation of the measured CN LIF spectrum indicates that the vibrational excitation of CN has increased; 52% of the CN products are formed in $v=0$, 34% in $v=1$, and 14% in $v=2$. The rotational excitation has decreased and the characteristic temperature parameters are $T(v=0)=900$ K, $T(v=1)=820$ K, and $T(v=2)=820$ K (see Table II).

In order to study the influence of the collision energy on the product state distribution a shorter photolysis wavelength was used. When Cl_2 is photodissociated at 308 nm instead of 355 nm, the available energy for the products in the reaction Cl+HCN(004) increases by 11 kJ mol^{-1} from 92 kJ mol^{-1} to 103 kJ mol^{-1}. However, this increase of energy in the collision complex has no significant effect on the CN product state distribution. This is also confirmed by the study of Crim and co-workers who used thermal Cl atoms to study the reaction with HCN(004).

In contrast to the reaction of HCN with two or four quanta of CH stretch being excited, a further increase of ν_3 excitation leads to a decrease of CN internal excitation. The simulation of the spectrum when highly excited HCN(105) is used as reactant indicates that 65% of the CN radicals are generated in $v=0$, 25% in $v=1$, and 10% in $v=3$. The rotational temperatures are $T(v=0)=740$ K, $T(v=1)=700$ K, and $T(v=2)=640$ K. Although the excitation energy of the (105) state is considerable higher than that of the (004) state, we obtained a significant change in the former tendency of increasing CN vibration with increasing H–C stretch excitation. The CN vibrational excitation decreases again, although one quantum of CN stretch has been excited in addition to 5 CH stretch quanta. The CN rotational excitation is slightly lower than in the Cl+HCN(004) reaction and much lower than in the reaction of Cl+HCN(002).

In order to study the influence of the CN stretching mode on the reaction dynamics, HCN is excited to the (302) state.

TABLE II. CN product state distributions from different HCN reactions. The vibrational distributions have an uncertainty of about ± 0.03 for $v=0,1$, and $v=2$.

Experiment	CN vibrational distribution, rotational temperature (K)					
	$P(v=0)$	T_{rot}/K	$P(v=1)$	T_{rot}/K	$P(v=2)$	T_{rot}/K
Cl_2+308 nm, HCN(002)	0.86	1700±45	0.13	940± 50	<0.01	
Cl_2+308 nm, HCN(004)	0.51	910±50	0.34	840± 40	0.15	740± 40
Cl_2+355 nm, HCN(004)	0.52	900±60	0.34	820± 50	0.14	820±160
Cl_2+355 nm, HCN(302)	0.45	820±61	0.43	760± 50	0.12	660±130
Cl_2+355 nm, HCN(105)	0.65	730±23	0.25	700± 70	0.10	640± 58
CH_3SH+266 nm, HCN(004)[a]	0.60		0.28		0.12	
CH_3SH+266 nm, HCN(004)	0.53	470±10	0.33	460± 15	0.14	450± 36
H_2S+193 nm, HCN(000)[b]	0.87	1404±95	0.13	1430±391	···	···
HBr+193 nm, HCN(000)[b]	0.81	1626±40	0.14	1645±137	0.05	···

[a]Thermal H atoms.
[b]Reference 4.

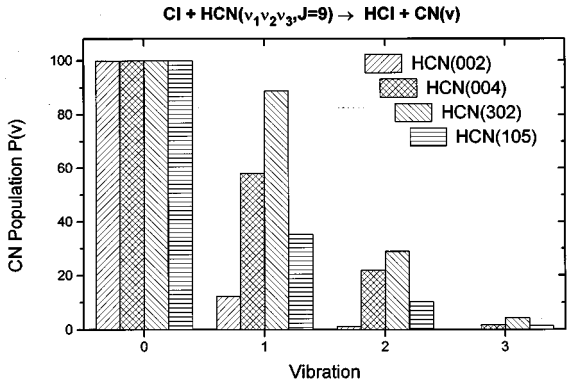

FIG. 3. Vibrational state distributions of CN produced in the reaction of chlorine atoms with vibrationally excited HCN($\nu_1 0 \nu_3$). The populations are normalized to $v=0$. Error bars are less than ± 7.

The reactions of chlorine atoms with HCN(302) and HCN(004) are isoenergetic, but in the former case only two quanta of CH stretch are excited and a significant part of energy ($3\nu_1$) is deposit in the CN stretch of HCN. Under the same experimental conditions the CN vibrational distribution of the reaction Cl+HCN(302)→HCl+CN(v,J) is slightly higher excited than in the reaction Cl+HCN(004). We observe 45% of the CN in $v=0$, 43% in $v=1$, and 12% in $v=2$. This result agrees very well with that recently obtained by Crim and co-workers.[26,27] The rotational temperatures are $T(v=0)=820$ K, $T(v=1)=760$ K, and $T(v=2)=660$ K (see Table II).

Figure 3 shows the CN vibrational product state distributions for all studied Cl+HCN reactions. The vibrational distributions are normalized to $v=0$ in order to gain a better insight into the influence of the HCN vibrational motion on the reaction.

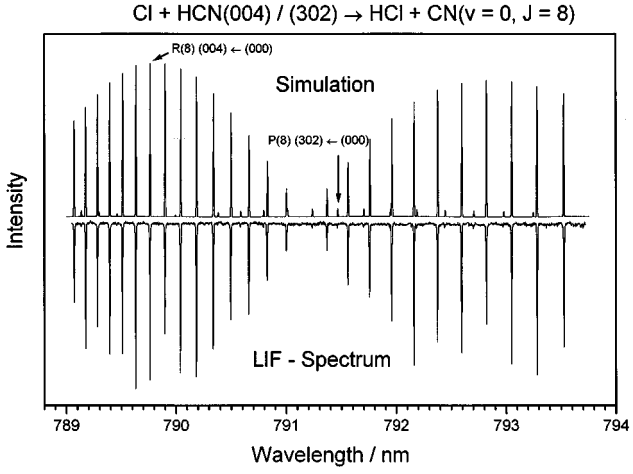

FIG. 4. Action spectrum of the Cl+HCN system. The CN probe laser is fixed at the $R(8)$ line and the HCN excitation laser is tuned around the (004)←(000) and (302)←(000) bands. Even the weak (302)←(000) excitation of HCN leads to CN products—although at a smaller rate, $k(004)/k(302)=2.8\pm 0.6$.

Since the excitation energies between the (004) and (302) states are nearly isoenergetic, it is relatively easy to measure an action spectrum of HCN in order to determine the reactivity of HCN(004) vs HCN(302). While the CN ($v=0$, $J=8$) product was monitored at a fixed wavelength via the $R(8)$ line, the HCN excitation laser light was tuned. Figure 4 shows the fluorescence signal (lower part) as a function of the excitation wavelength and a simulation (upper part) using the known HCN Franck–Condon and Hönl–London factors.[12] In principle, one can compare the LIF intensities from the action spectrum with those from the photoacoustic spectrum in order to obtain information on the relative reactivity without knowledge of the transition probabilities. However, we observe a nonlinear dependence of the photoacoustic spectrum from the strength of the transitions and from the HCN pressure. Therefore, the LIF intensities are compared with the corresponding intensities from the simulation. We find a ratio of rate constants between HCN(004) and HCN(302) of $k(004)/k(302)=2.8\pm 0.6$. Thus, the reaction of Cl with HCN is faster when the energy is located in the reaction coordinate (the CH stretch) instead of locating the same amount of energy in three quanta of CN and two quanta of CH stretch.

The same method was used to analyze the influence of the HCN bending vibration, ν_2, on the reactivity with chlorine. The CN product was also monitored via the $R(8)$ line and the HCN excitation laser light was tuned in the range of the (105)←(000) Σ–Σ and the (11^15)←(01^10) Π–Π transitions. Since both bands are observable in the action spectrum with intensities which are comparable with the simulation, we conclude that both reactions proceed at comparable rates. Summation over all observed rotational lines in the action spectrum within the wavelength range of 572 nm and 574 nm leads to a reaction rate ratio of $k(11^15):k(105)=0.8\pm 0.2$. Thus, additional excitation of the bending mode by one quantum does not lead to a significant change of the reactivity. However, it should be mentioned that the reaction rate of Cl+HCN(105) is already close to the gas kinetic limit which was roughly estimated by comparing the intensity of the signal with the sensitivity of the apparatus known from various dissociation experiments.[28]

C. H+HCN(ν_1,ν_2,ν_3)

The reaction of hydrogen atoms with HCN in the (004) and in the (302) state was investigated with H atoms being generated in the photodissociation of CH_3SH. Figure 5 shows the excitation spectrum of CN obtained from the reaction H+HCN(004)→H_2+CN(v,J). The corresponding simulation yields 53% of the radicals being formed in $v=0$, 33% in $v=1$, and 14% in $v=2$. The rotational distributions in $v=0$, 1 and 2 are characterized by temperatures of 470 K, 460 K, and 450 K, respectively (Table II). Compared to the Cl reaction, the reaction of H atoms with HCN(004) leads to less rotationally excited CN products. However, the vibrational distribution of CN does not significantly change, when hydrogen atoms are used instead of chlorine atoms.

Since the collision energy is relatively high due to the

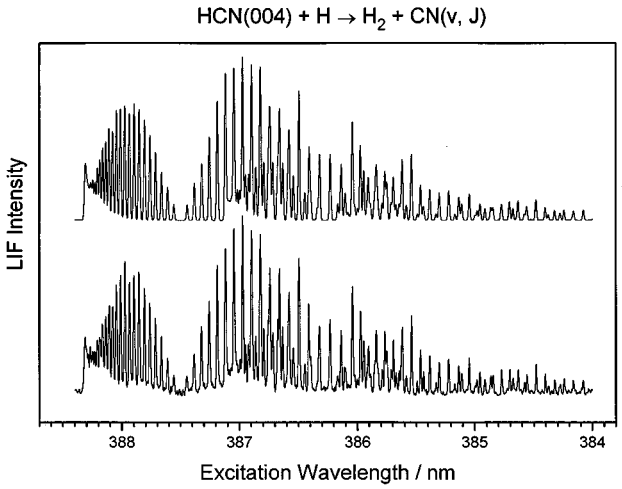

FIG. 5. Laser induced fluorescence spectrum of CN generated in the reaction of hydrogen atoms with HCN with 4 CH stretch quanta of HCN being excited (lower part). For an evaluation of the experimental spectrum a simulation of the spectrum has been performed (upper part).

high recoil velocity of the H atom, the CN vibrational excitation may be caused by translational energy of the H+HCN reaction system and not by initial vibrational energy of HCN. To ensure that the vibrational excitation of the CN product is mainly a result of the initial internal excitation of HCN, we cooled the translationally excited H atoms by adding He to the MeSH/HCN mixture. Figure 6 shows three CN spectra with different ratios of pressures $p(\mathrm{He})/p(\mathrm{HCN})=0$, 30, and 80. Since the cooling gas helium is very efficient in quenching the speed distribution of hydrogen atoms—the H atom velocity is equilibrated within less than 10 collisions[29]—the ratio $p(\mathrm{He})/p(\mathrm{HCN})=80$ is sufficient to obtain thermal H atoms. No significant change of the vibrational state distribution is observable. At the highest ratio $p(\mathrm{He})/p(\mathrm{HCN})=80$, we found 60% of all CN in $v=0$, 28% in $v=1$, and 12% in $v=2$ (Table II). The observed CN rotational temperature, (290 ± 15) K, is close to room temperature as expected because the CN rotation is already relaxed at these collision rates.

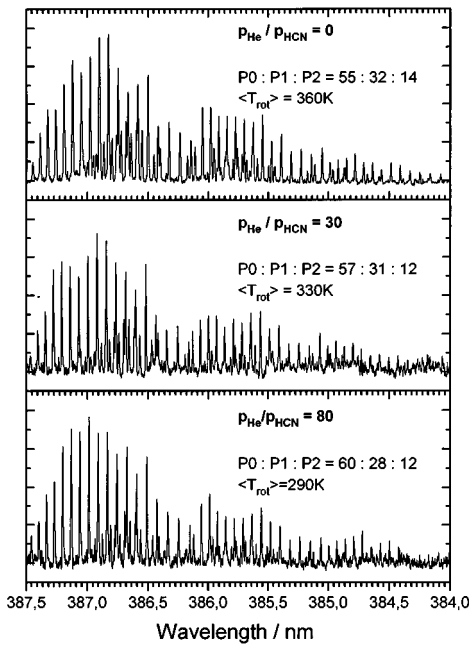

FIG. 6. Spectrum of the CN product molecule generated in the reaction of H+HCN(004). Helium as buffer gas has been added in order to relax the initially hot hydrogen atom.

An action spectrum of the reaction $\mathrm{H+HCN}(\nu_1 0 \nu_2)\rightarrow \mathrm{H_2+CN}$ is obtained by monitoring the $\mathrm{CN}(v=0,\ J=8)$ product as a function of HCN excitation. Only rotational lines from the (004)←(000) excitation are detected. No transitions which can be attributed to the (302)←(000) excitation of HCN are observable under the present experimental conditions. Using the S/N ratio and the Hönl–London factors of both transitions, (302)←(000) and (004)←(000), we estimate a maximum ratio of rate constants of $k_{004}/k_{302}>4$. Therefore, the reactivity of H+HCN has to be mode specific.

The energetics of all studied HCN reactions are listed in Table III. For each reaction the collision energy, the internal energy of HCN, the available energy, and the energy release in the CN product are listed. In addition, results from reactions of fast H atoms with HCN(000) are also given.

IV. DISCUSSION

A. Cl+HCN(ν_1,ν_2,ν_3)

In general, channeling energy into the reaction coordinate will increase the reaction rate while energy stored in a coordinate perpendicular to the reaction coordinate will have no or minor influence on the reactivity. Since the CH bond is the one which has to break, it is understandable that the reaction rate increases when $4\nu_3$ quanta of CH stretch and no ν_1 quantum of CN stretch are excited instead of $2\nu_3$ and $3\nu_1$ quanta ($k_{004}/k_{302}=2.8\pm0.5$). However, from the experimental results it is obvious that CN does not act as a spectator because the CN product is vibrationally excited. Roughly 18% of the available energy are released as vibrational energy (Table III). This energy release is essentially independent of the initially excited vibrational modes of HCN (002, 004, 302) and, thus, the reaction process is predominantly described by intermediate complex formation, where sufficient time is left for an energy distribution between all degrees of freedom. The CN vibrational state distribution is not caused by the collision energy of the photolytically produced Cl atoms because the use of different photolysis wavelengths has no significant effect on the CN product state distribution. This is also confirmed by measurements of thermalized Cl atoms.[26,27]

When five quanta of CH stretch and one quanta of CN stretch are excited, then the CN vibrational excitation decreases significantly ($f_{\mathrm{vib}}=8\%$). This behavior is expected for a more direct reaction, A+BCD→AB+CD where the ''old'' CD bond does not participate in the reaction. For example, the reaction of HCN with translationally hot OH radi-

TABLE III. Partition of internal CN product energies from different HCN reactions. The reaction enthalpy for Cl+HCN→HCl+CN is $\Delta_r H^0(0\ \mathrm{K})=94\ \mathrm{kJ\ mol^{-1}}$ and for H+HCN→H_2+CN is $\Delta_r H^0(0\ \mathrm{K})=90\ \mathrm{kJ\ mol^{-1}}$. E_{av} is the available energy equal to $E_{coll}+E_{int}-\Delta_r H^0$. E_{int} is the internal vibrational and rotational energy of HCN equal to $E_{int}=E_{vib}+BJ'(J'+1)$, $J'=9$. $f_{vib}=E_{vib}/E_{av}$, $f_{rot}=E_{rot}/E_{av}$, $f_{int}=E_{int}/E_{av}$.

Experiment	Energy reactants/kJ mol^{-1}			CN product energies				
	E_{coll}	E_{int}	E_{av}	E_{rot}	E_{vib}	$f_{rot/\%}$	$f_{vib/\%}$	$f_{int/\%}$
Cl_2+308 nm, HCN(002)	36	79	21	13.3	3.7	63	18	81
Cl_2+308 nm, HCN(004)	36	152	94	7.2	15.6	8	17	25
Cl_2+355 nm, HCN(004)	25	152	83	7.2	15.3	9	18	27
Cl_2+355 nm, HCN(302)	25	152	83	6.5	16.3	8	20	28
Cl_2+355 nm, HCN(105)	25	211	142	6.0	11.0	4	8	12
CH_3SH+266 nm, HCN(004)	4	152	66	(3)[b]	12.7	4	19	23
CH_3SH+266 nm, HCN(004)	80	152	142	3.8	14.9	3	10	13
H_2S+193 nm, HCN(000)[a]	222	3	135	11.7	3.2	9	2	11
HBr+193 nm, HCN(000)[a]	243	3	156	12.9	5.8	8	4	12

[a]Reference 4.
[b]Estimated from the reaction of HCN(004) with hot hydrogen.

cals generates CN product molecules exclusively in the vibrational ground state. Another example is the reaction of $O(^1D)$ with H_2O where the two generated OH radicals which show a different internal excitation.[30] While one OH product molecule is vibrationally excited (the "new" OH bond), the partner molecule is formed essentially in the vibrational ground state.[31]

The different vibrational energy release in the reactions Cl+HCN[(002), (302), (004)] and Cl+HCN(105) indicates a change in the reaction dynamics. While at the highest internal excitation (105) the reaction proceeds rather directly, at all other internal excitations the behavior becomes more typical for a long living collision complex.

We performed an analysis of the reaction mechanism by using phase space theory (PST),[32–34] because this theory imposes only the conservation laws on the reaction, but no specific internal motions of the complex are related to motions of the products. The distribution of the collision energy $f(E_{coll})$ was incorporated in the calculations by using up to 17 different values of E_{coll} with $f(E_{coll})$ as appropriate weight. The initial and the final orbital angular momentum is constrained according to $0 \leqslant L \leqslant L_{max}=\mu.\ b\cdot v_{rel}$, where μ is the reduced mass of the product system (H+HCN or H_2+CN), b the impact parameter, and v_{rel} the relative velocity of the fragments. v_{rel} is given by the equation $v_{rel}=\sqrt{2E/\mu}$ using $E=E_{coll}$ for the initial velocity, and $E=E_{av}-E_{int}$(products) for the final velocity of the products. By using different impact parameters b, the degree of constraint of the orbital angular momentum can be varied in a wide range. We find that the rotational distribution is sensitive on b, while the vibrational distribution shows no significant changes.

The results of the calculations are shown in Table IV. A comparison with the experimental results (Table I) shows the vibrational distribution can be reproduced fairly well—HCN(105) expected. The calculated CN vibrational distributions in the reaction Cl+HCN are slightly colder than the experimental ones. Significant differences are obtained in the calculated and the observed rotational distributions. When only two quanta of CH stretch are excited, then PST predicts a lower rotational excitation of the CN product than that observed in the experiment. At higher HCN excitations a much higher rotational excitation is expected if PST can be applied. In order to match the calculated PST distribution

TABLE IV. PST-calculations.

Experiment	$b_0=b_1$	CN vibrational distribution, rotational temperature (K)					CN product energies	
		$P(v=0)$	$P(v=1)$	$P(v=2)$	$P(v=3)$	$P(v=4)$	E_{rot}	E_{vib}
Cl_2+308 nm, HCN(002)	0.5	0.94	0.06	⋯	⋯	⋯	7.5	1.6
	1.0	0.95	0.05	⋯	⋯	⋯	8.9	1.3
Cl_2+355 nm, HCN(004)	0.3	0.60	0.28	0.10	0.02	⋯	6.9	13.1
	1.0	0.64	0.27	0.08	0.01	⋯	16.4	11.1
Cl_2+355 nm, HCN(105)	0.1	0.42	0.27	0.17	0.09	0.04[b]	5.5	26.5
	1.0	0.46	0.28	0.16	0.07	0.03	22.9	23.2
CH_3SH+266 nm, HCN(004)[a]	0.5	0.67	0.28	0.05	⋯	⋯	2.6	9.3
	1.0	0.66	0.28	0.06	⋯	⋯	4.0	9.8
CH_3SH+266 nm, HCN(004)	0.5	0.43	0.28	0.16	0.08	0.04[b]	4.6	25.5
	1.0	0.44	0.28	0.16	0.08	0.03[b]	9.2	25.0

[a]Thermal H atoms.
[b]$P(v=5)=0.01$.

with the experimental results of the HCN(004) and HCN(302) reactions the impact parameter must be restricted to values below 0.3 Å.

The differences in the CN state distributions between PST and the experiment suggest that the reaction Cl +HCN→HCl+CN cannot completely be described by a statistical process. It seems to be more likely that the product rotational state distribution is also influenced by final state interaction. Especially in the reaction with HCN(105) the collision complex may not live long enough to allow internal energy randomization prior to dissociation into the HCl and CN fragments. As a consequence the reaction proceeds rather directly and only small amounts of energy are stored in the nonreactive CN coordinate.

B. H+HCN(ν_1,0,ν_3)

We also performed phase space calculations for this reaction as described before. When comparing the results of PST (Table IV) with those from the experiment it is obvious that the theoretical model is not adequate to describe the reaction mechanism. Both the vibrational and the rotational distributions are colder than expected from the statistical theory. Furthermore, we observe a strong mode specific behavior of the reactivity. When HCN(004) is used instead of HCN(302), the reaction rate increases by a factor of at least 4. Vibrational motion along the reaction coordinate (ν_3) enhances reactivity whereas motion perpendicular to the reaction coordinate (ν_1) hinders reactivity or is ineffective. The reaction H+HCN cannot totally be described by a spectator model, because a significant part of the available energy is released as CN vibrational energy.

The reaction of hydrogen atoms with HCN(004) produces CN with a vibrational distribution similar to the reaction with chlorine. When using thermal H atoms roughly 19% of the available energy are located in the CN vibrational mode (Table III). The increase of collision energy by using photolytic H atoms has no significant effect on the observed vibrational distribution of the CN fragment. Thus, the vibrational excitation of CN should not be a consequence of using fast H atoms with high translational energy. This result agrees with those obtained by Lambert *et al.*,[35] who analyzed the reaction of translationally hot H atoms with thermal HCN (Tables II and III). Precursors of the H atoms were H_2S and HBr, photolyzed at 193 nm. This leads to available energies of 132 kJ/mol and 153 kJ/mol for the products, which are in the range of the presente reaction H+HCN(004). The observed CN state distribution in the hot H atom reaction is characterized by a relatively high rotational and low vibrational energy release.

When vibrationally excited HCN is used in the reaction with hydrogen atoms then a low rotational excitation of the CN product is observed. Only 3% of the available energy are located in this degree of freedom. The best fit of the CN rotational energies by PST is obtained when the impact parameter b is restricted to a value of 0.5 Å.

In summary, one can exclude the pure spectator model for the reaction of H with HCN as well as for the reaction of chlorine atoms with HCN. In the case of Cl+HCN the CN is predominantly formed by dissociation of an intermediate complex. However, a slightly higher CN product vibrational excitation is observed when the CN stretch in HCN is excited ($3\nu_{CN}+2\nu_{CH}$) instead of a pure CH stretch excitation ($4\nu_{CH}$). The reaction mechanism changes from complex formation towards a more direct reaction when the (105) band is excited. In case of the hydrogen atom reaction, H+HCN(004), an intermediate complex formation is very important for the dynamics of that reaction.

ACKNOWLEDGMENTS

We thank Professor Fleming F. Crim and Joann M. Pfeiffer for useful discussions and for communicating their results prior to publications. We also like to thank Professor Franz J. Comes for helpful discussions and material support. C. K. thanks the Fonds der Chemischen Industrie for fellowship support. Financial support by Deutsche Forschungsgemeinschaft is gratefully acknowledged.

[1] M. J. Frost, I. W. Smith, and R. D. Spencer-Smith, Chem. Soc. Faraday Trans. **89**, 2355 (1993).
[2] I. R. Sims and I. W. M. Smith, J. Chem. Soc. Faraday Trans. II **85**, 915 (1989).
[3] H. Schacke, H. Gg. Wagner, and J. B. Wolfrum, Ber. Bunsenges. Phys. Chem. **81**, 670 (1977).
[4] H. M. Lambert, T. Carrington, S. V. Filseth, and C. M. Sadowski, J. Phys. Chem. **97**, 128 (1993).
[5] R. A. Bair and T. H. Dunning, Jr., J. Chem. Phys. **82**, 2280 (1985).
[6] I. R. Sims and I. W. M. Smith, Chem. Phys. Lett. **149**, 565 (1988).
[7] Q. Sun and J. M. Bowman, J. Chem. Phys. **92**, 5201 (1990).
[8] H. Sasada, J. Chem. Phys. **88**, 767 (1988).
[9] K. R. German and W. S. Gornall, J. Opt. Soc. Am. **71**, 1452 (1981).
[10] A. M. Smith, S. L. Coy, and W. Klemperer, J. Mol. Spectrosc. **134**, 134 (1989).
[11] D. H. Rank and G. Skrinko, J. Opt. Soc. Am. **50**, 421 (1960).
[12] A. M. Smith and U. G. Jørgensen, J. Chem. Phys. **87**, 5649 (1987).
[13] A. E. Douglas and D. Sharma, J. Opt. Soc. Am. **21**, 448 (1953).
[14] D. Romanini and K. K. Lehmann, J. Chem. Phys. **102**, 633 (1995).
[15] D. Romanini and K. K. Lehmann, J. Chem. Phys. **99**, 6287 (1993).
[16] A. P. Baronavski, Chem. Phys. Lett. **61**, 532 (1979).
[17] G. L. Vaghjiani, J. Chem. Phys. **99**, 5936 (1993).
[18] S. H. S. Wilson, M. N. R. Ashfold, and R. N. Dixon, J. Chem. Phys. **101**, 7538 (1994).
[19] S. B. Barone, A. A. Turnipseed, T. Gierczak, and A. R. Ravishankara, J. Phys. Chem. **98**, 11 969 (1994).
[20] J. L. Kinsey, Annu. Rev. Phys. Chem. **28**, 9, 34 (1978).
[21] W. Demtröder, *Laser Spectroscopy* (Springer, Berlin, 1982), p. 417.
[22] P. J. Chantry, J. Chem. Phys. **55**, 2746 (1971).
[23] W. J. van der Zande, R. Zhang, R. N. Zare, K. G. McKendrick, and J. J. Valentini, J. Phys. Chem. **95**, 8205 (1991).
[24] S. H. S. Wilson, M. M. N. Ashfold, and R. N. Dixon, J. Chem. Phys. **101**, 7538 (1994).
[25] E. Jensen, J. S. Keller, G. C. G. Waschewsky, J. E. Stevens, R. L. Graham, K. F. Freed, and L. J. Butler, J. Chem. Phys. **98**, 2882 (1993).
[26] J. M. Pfeiffer, R. B. Metz, J. D. Thoemke, E. Woods III, and F. F. Crim, J. Chem. Phys. **104**, 4490 (1996).
[27] R. B. Metz, J. D. Thoemke, J. M. Pfeiffer, and F. F. Crim, Chem. Phys. Lett. **221**, 347 (1994).
[28] K. Mikulecky and K.-H. Gericke, J. Chem. Phys. **101**, 9635 (1994).
[29] We have done calculations using equations from G. Nem and P. L. Housten, J. Chem. Phys. **97**, 7865 (1992).
[30] Discrimination between the two products is possible by isotopic labeling of the O(^1D) atom.

[31] K.-H. Gericke, F. J. Comes, and R. D. Levine, J. Chem. Phys. **74**, 6106 (1981); F. J. Comes, K.-H. Gericke, and J. Manz, *ibid*. **75**, 2853 (1981); D. G. Sander, J. C. Stephenson, D. S. King, and M. P. Casassa, *ibid*. **97**, 952 (1994); C. B. Cleveland and J. R. Wiesenfeld, *ibid*. **96**, 248 (1992).
[32] P. Pechukas and J. C. Light, J. Chem. Phys. **42**, 3281 (1965).
[33] P. Pechukas and J. C. Light, J. Chem. Phys. **44**, 794 (1966).
[34] J. R. Beresford and G. Hancock, Faraday Discuss. Chem. Soc. **75**, 211 (1983).
[35] H. M. Lambert, T. Carrington, S. V. Filseth, and C. M. Sadowski, J. Phys. Chem. **97**, 128 (1993).